H1prelim-03-043

Determination of F_L at low Q^2

H1 Collaboration

Abstract

An extraction of logitudinal structure function $F_L(x, Q^2)$ from H1 data at low $Q^2 \sim 1$ GeV is reported. The analysis is based on the data collected in 1999 in a dedicated low Q^2 running period and in 2000 during shifted vertex runs. Two methods of $F_L(x, Q^2)$ extraction are discussed. It is shown that results from both methods are consistent. Theoretical predictions are compared to the extracted $F_L(x, Q^2)$ points. The $F_L(x, Q^2)$ determination by H1 experiment in the whole Q^2 range is summarised.

Prepared for DIS 2003, St. Petersburg

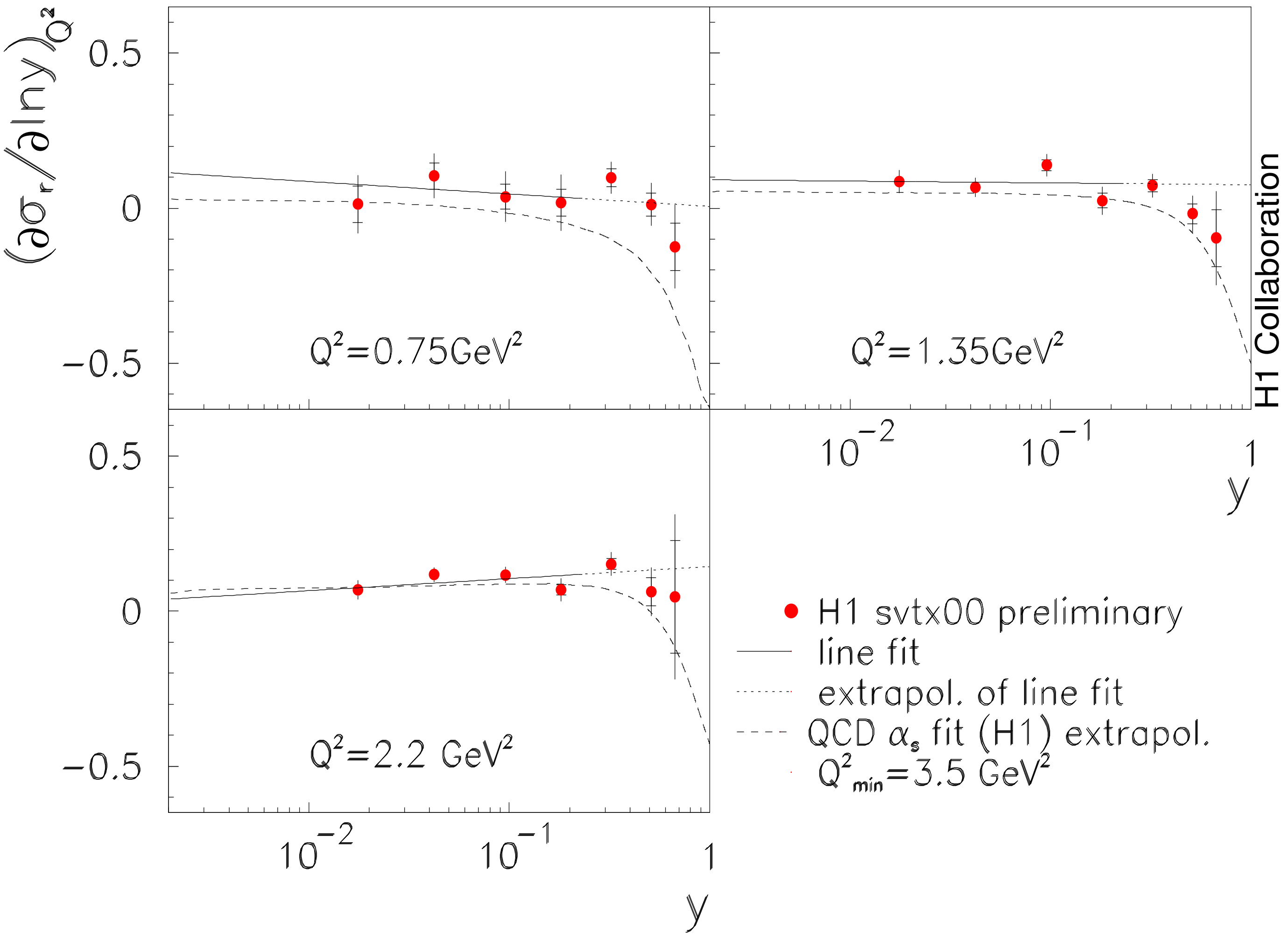

Figure 1: Derivative of $\sigma_\mathbf{r}$ at fixed Q^2. Inner error bars correspond to statistical errors. Total errors include statistical, uncorrelated and systematic errors added in quadrature. A linear fit to the low y points and its extrapolation to the high y region is shown. In the 'derivative' method, F_L is extracted from the deviation from the linear behaviour in the high y region according to $\partial\sigma_r/\partial \ln y = \partial F_2/\partial \ln y - y^2(2-y)/Y_+^2 F_L$, under the assumption that the linear behaviour of $\partial F_2/\partial \ln y$ persists in the high y region.

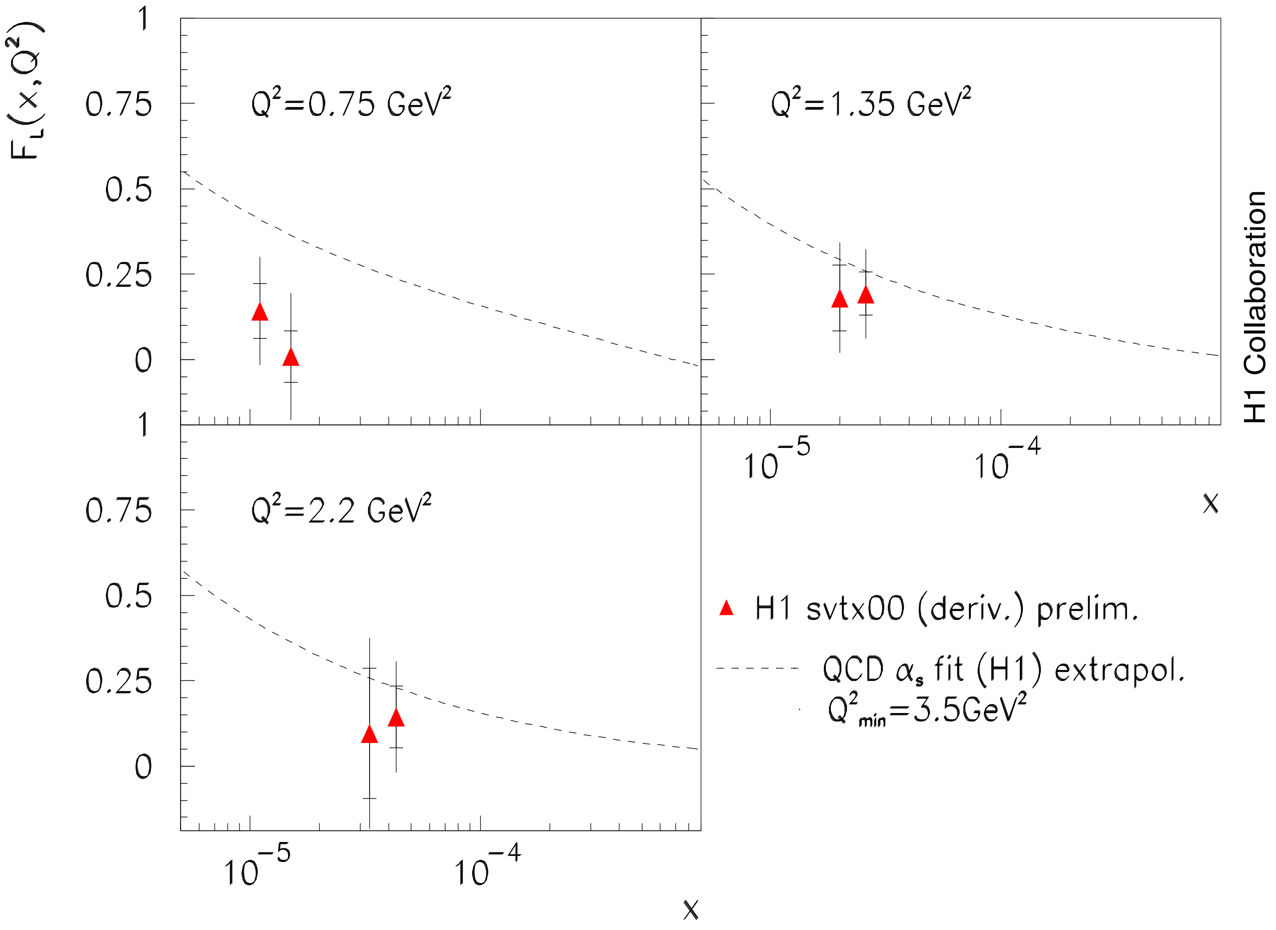

Figure 2: $F_L(x, Q^2)$ (for fixed Q^2) from 2000 shifted vertex data as extracted by derivative method. Inner error bars correspond to statistical errors. Total errors include statistical, uncorrelated and systematic errors added in quadrature.

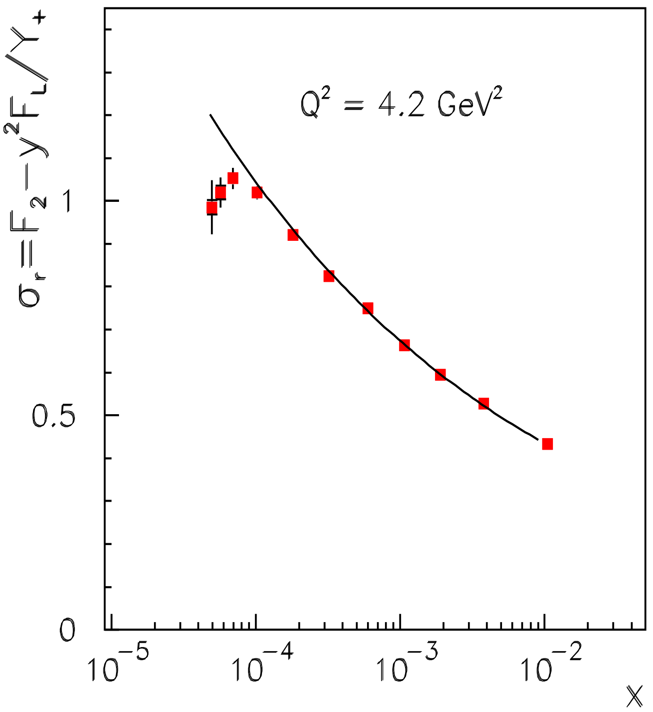

Figure 3: The x distribution of reduced cross section for $Q^2 = 4.2$ GeV^2. A fit of the form $\sigma_r = c \cdot x^{-\lambda}$ to the high x data is shown. The deviation from this behaviour at low x (high y) is due to the F_L term. The data used on this plot were colleced during 1999 binimum bias running period.

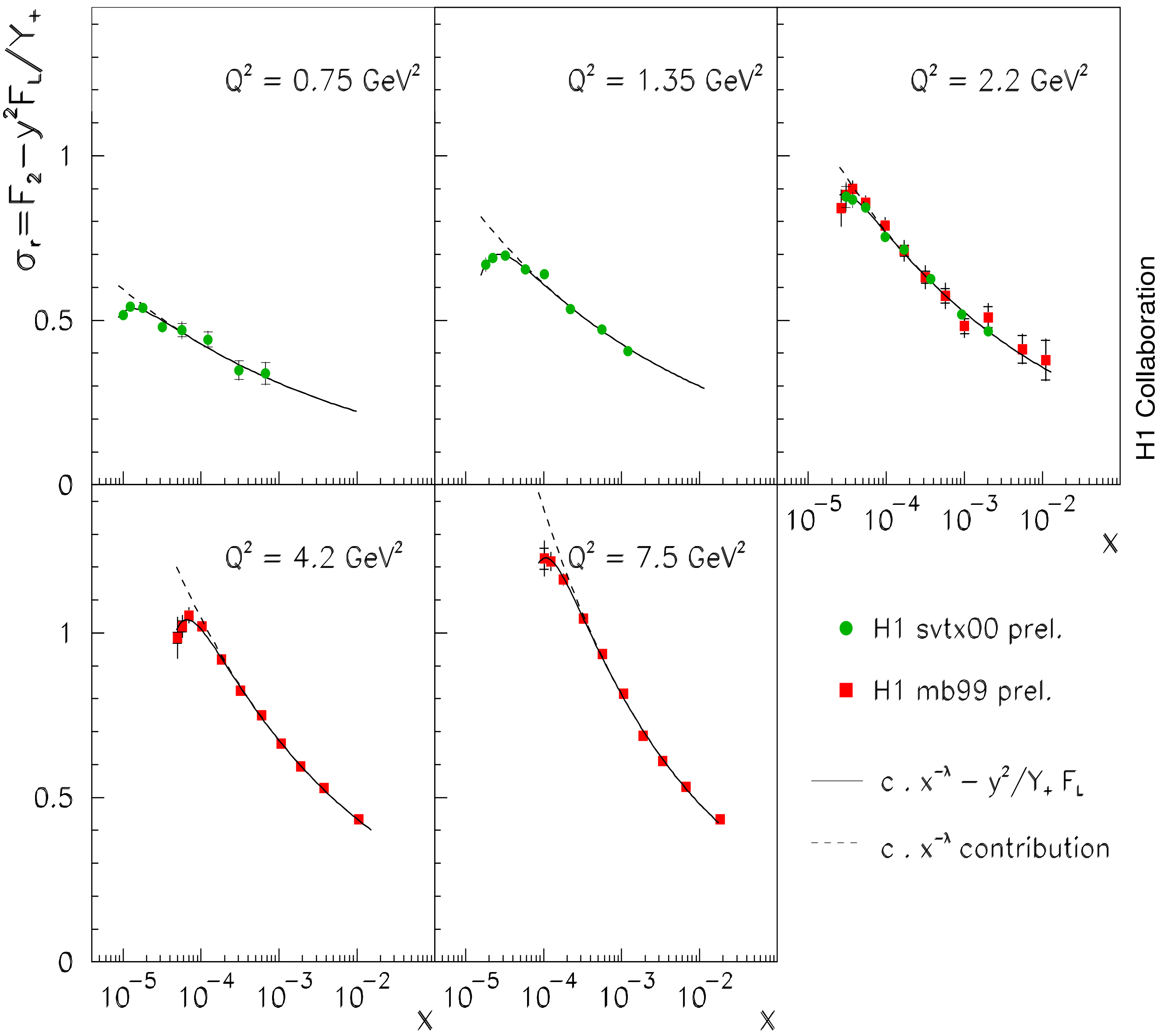

Figure 4: The reduced cross section as a function of x for different Q^2 bins. Data from 1999 minimum bias and 2000 shifted vertex running periods shown. Inner error bars correspond to statistical errors. Total errors include statistical, uncorrelated and systematic errors added in quadrature. The dashed lines show fits of the form $\sigma_r = c \cdot x^{-\lambda}$. The solid lines show fits of the form $\sigma_r = c \cdot x^{-\lambda} - y^2/Y_+ F_L$, from which F_L is extracted in the 'shape' method.

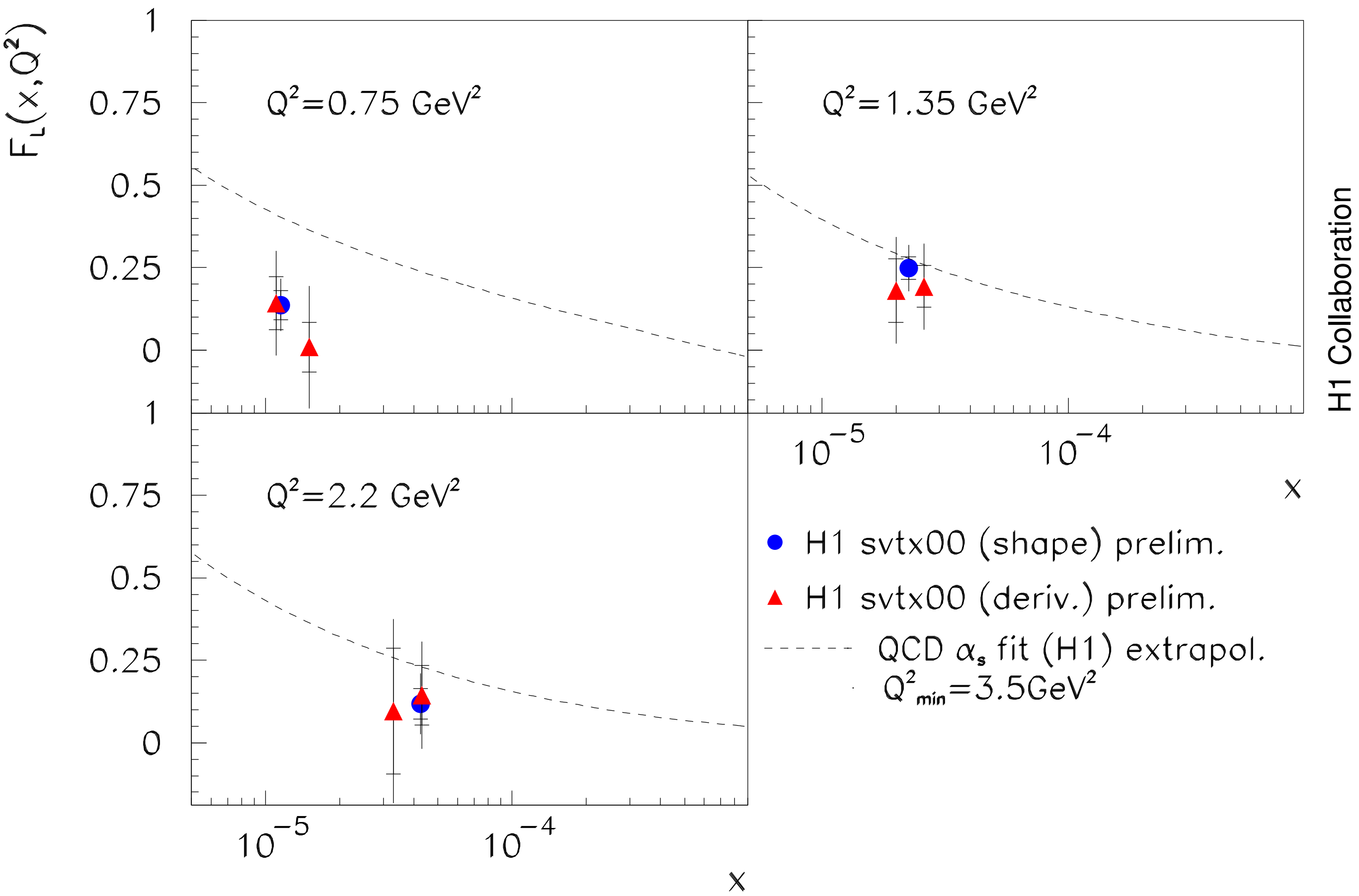

Figure 5: Comparition of $F_L(x, Q^2)$ results (for fixed Q^2) from 2000 shifted vertex data as extracted by the derivative and shape methods. The inner error bars correspond to statistical errors. Total errors include statistical, uncorrelated and systematic errors added in quadrature.

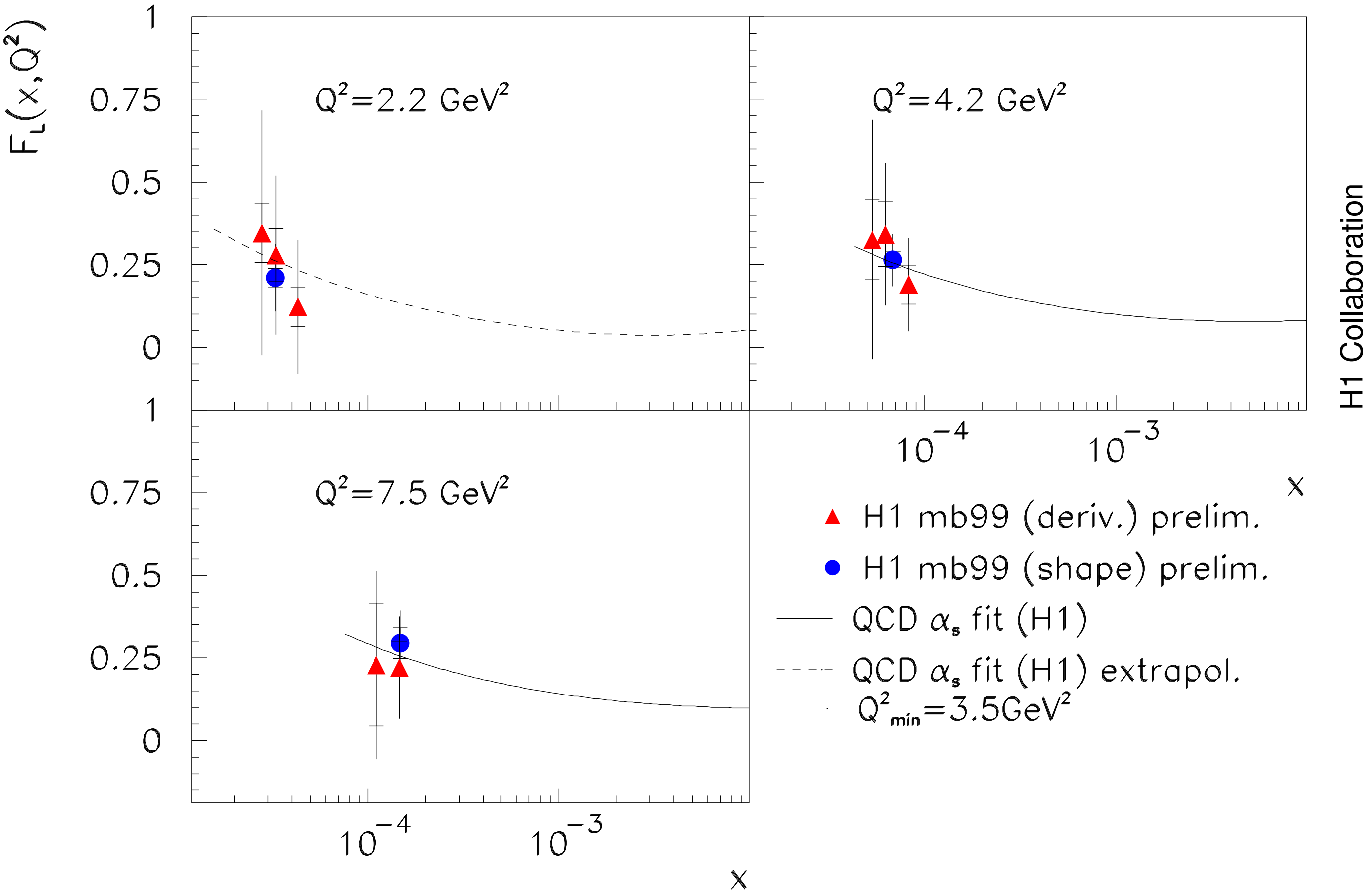

Figure 6: Comparition of $F_L(x, Q^2)$ results (for fixed Q^2) from 1999 minimum bias data as extracted by derivative and shape methods. Inner error bars correspond to statistical errors. Total errors include statistical, uncorrelated and systematic errors added in quadrature.

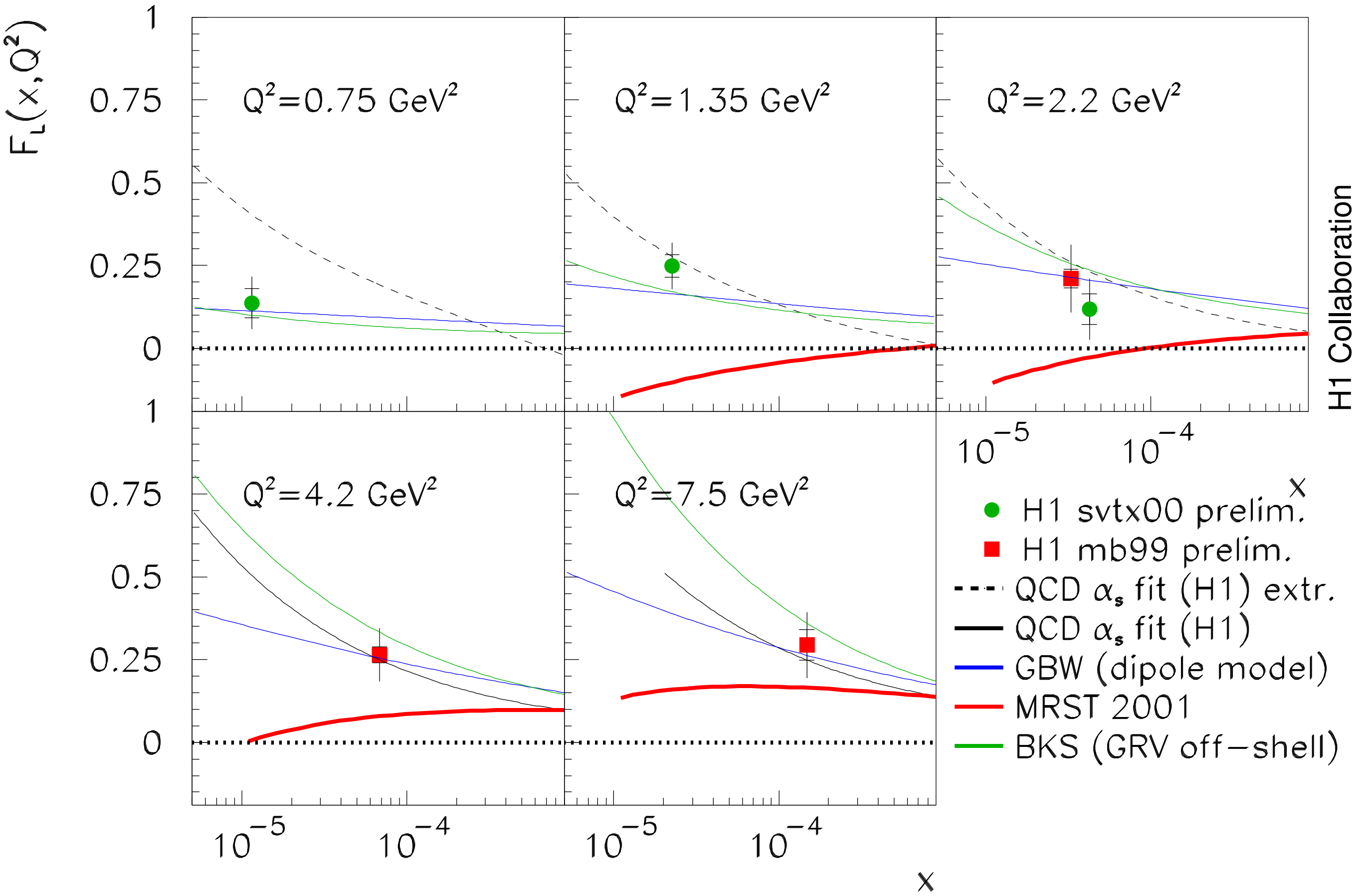

Figure 7: $F_L(x, Q^2)$ extraction for fixed Q2 from 1999 minimum bias and 2000 svtx. data as extracted by the shape method. Inner error bars correspond to statistical errors. Total errors include statistical, uncorrelated and systematic errors added in quadrature. The curves show predictions of different theoretical models.

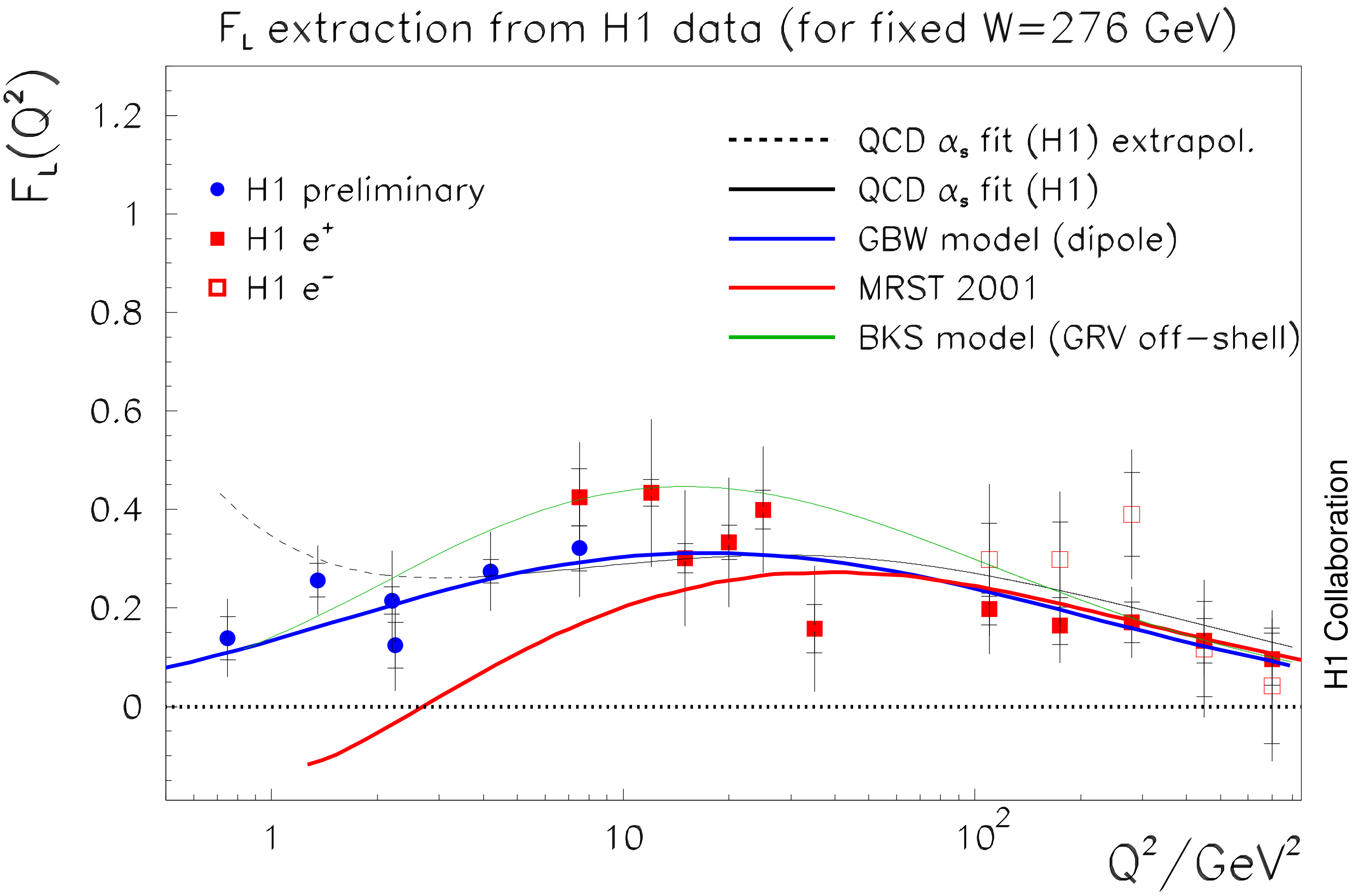

Figure 8: Q^2 dependence of $F_L(x, Q^2)$ (at fixed W=276 GeV), summarising all data from the H1 experiment. Inner error bars correspond to statistical errors. Total errors include statistical, uncorrelated and systematic errors added in quadrature. The curves show predictions of different theoretical models.